

Synchronization and phase ordering in globally coupled chaotic maps

O. Alvarez-Llamoza¹ and M. G. Cosenza²

¹*Departamento de Física, FACYT, Universidad de Carabobo, Valencia, Venezuela*

²*Centro de Física Fundamental, Universidad de Los Andes, Mérida, Venezuela*

We investigate the processes of synchronization and phase ordering in a system of globally coupled maps possessing bistable, chaotic local dynamics. The stability boundaries of the synchronized states are determined on the space of parameters of the system. The collective properties of the system are characterized by means of the persistence probability of equivalent spin variables that define two phases, and by a magnetization-like order parameter that measures the phase-ordering behavior. As a consequence of the global interaction, the persistence probability saturates for all values of the coupling parameter, in contrast to the transition observed in the temporal behavior of the persistence in coupled maps on regular lattices. A discontinuous transition from a non-ordered state to a collective phase-ordered state takes place at a critical value of the coupling. On an interval of the coupling parameter, we find three distinct realizations of the phase-ordered state, which can be discerned by the corresponding values of the saturation persistence. Thus, this statistical quantity can provide information about the transient behaviors that lead to the different phase configurations in the system. The appearance of disordered and phase-ordered states in the globally coupled system can be understood by calculating histograms and the time evolution of local map variables associated to these collective states.

PACS numbers: 89.75.Fb, 87.23.Ge, 05.50.+q

I. INTRODUCTION.

Globally coupled systems have been a research topic receiving a large amount of attention because of their applicability to a variety of contexts. The dynamical elements in such systems are subject to a common interaction field. Global interactions arise in the description of many physical, biological, chemical and social systems, such as Josephson junction arrays [1], multimode lasers [2], coupled oscillators [3, 4], charge density waves [5], parallel electric circuits, neural dynamics, ecological systems, evolution models [6], economic exchange [7], social networks [8], mass media models [9], cross-cultural interactions [10], etc. Global interactions also play a relevant role in models of many systems driven by long-range interactions, able to generate strong correlations between highly interconnected elements. Systems with global interactions can exhibit a variety of phenomena, such as chaos synchronization, nontrivial collective behavior, dynamical clustering, chaotic itineracy [6, 11], quorum sensing [12], etc. These behaviors have been experimentally investigated in arrays of globally coupled oscillators in several systems [13–17].

In addition to these phenomena, the description of generic effects associated to the presence of global coupling in dynamical processes in complex systems is still an open problem. In this respect, globally coupled maps [18] constitute paradigmatic models for the study of dynamical systems with global interactions. Spatial concepts lose meaning and only temporal properties become relevant in globally coupled maps. These characteristics should introduce new features in many processes that have been investigated in spatially extended systems with short range interactions.

In particular, there has been much interest in the study of the phase-ordering properties of systems of coupled bistable maps and their relationship with Ising models in statistical physics [19–28]. These works have mainly assumed the phase competition dynamics taking place on networks with local interactions.

In this article we investigate the collective behavior of a system of globally coupled bistable chaotic maps, including the occurrence of synchronized states and the phenomenon of phase competition. This model provides a scenario to compare the roles that local and global interactions play on the occurrence of phase growth and phase transitions on spatiotemporal systems. In Sec. (II) we present the model of globally coupled maps and describe local dynamics that exhibits bistable, chaotic behavior. In Sec. (III) we determine analytically the stability condition for synchronized states on the space of parameters of the system. The phase-ordering properties associated to the collective dynamics of the system are studied in Sec. (IV) by employing appropriate statistical quantities. Section (V) contains the conclusions of this work.

II. GLOBALLY COUPLED BISTABLE CHAOTIC MAPS.

We consider a globally coupled map system defined by

$$x_{t+1}^i = (1 - \varepsilon)f(x_t^i) + \frac{\varepsilon}{N} \sum_{j=1}^N f(x_t^j), \quad (1)$$

where x_t^i describes the state variable of element i ($i = 1, 2, \dots, N$), at discrete time t , the parameter ε measures the coupling strength between the elements, and $f(x)$ is a map that expresses the local dynamics. The term expressing the global coupling between the maps corresponds to the mean field of the system. In this article, we employ a system size $N = 10^5$.

The local dynamics is given by a piecewise linear, odd map

$$f(x) = \begin{cases} -2\mu/3 - \mu x, & \text{if } x \in [-1, -1/3], \\ \mu x, & \text{if } x \in [-1/3, 1/3], \\ 2\mu/3 - \mu x, & \text{if } x \in [1/3, 1], \end{cases} \quad (2)$$

where the local parameter $\mu \in [-3, 3]$ and $x \in [-1, 1]$. For $\mu = 3$, $f(x)$ becomes the chaotic map introduced by Miller and Huse [19]. For $\mu \in [-1, 1]$, the map possesses the stable fixed point $f(x^*) = x^* = 0$. When the parameter $\mu \in (1, 2)$, the local map is chaotic and bistable: there are two symmetric chaotic band attractors, corresponding to the invariant intervals $I^\pm = [\pm\mu(2 - \mu)/3, \pm\mu/3]$, and separated by a finite gap about the origin. This map has been shown to exhibit phase-ordering properties on locally coupled map lattices [21, 22].

III. SYNCHRONIZED STATES.

The coupled map system Ec. (1) can be expressed in vector form as

$$\mathbf{x}_{t+1} = (1 - \varepsilon)\mathbf{f}(x_t) + \frac{\varepsilon}{N}\mathbf{M}\mathbf{f}(x_t) = \left[(1 - \varepsilon)\mathbf{I} + \frac{\varepsilon}{N}\mathbf{M} \right] \mathbf{f}(x_t), \quad (3)$$

where \mathbf{x}_t and $\mathbf{f}(x_t)$ are N -dimensional vectors with components $[\mathbf{x}_t]_i = x_t^i$ and $[\mathbf{f}(x_t)]_i = f(x_t^i)$, respectively; \mathbf{I} is the $N \times N$ identity matrix; and \mathbf{M} is an $N \times N$ matrix expressing the coupling between the elements. For the global coupling, Ec. (1), all the components of \mathbf{M} are equal to 1.

A synchronized state occurs when $x_t^i = x_t^j$, $\forall i, j$. From the linear stability analysis of synchronized states in coupled map lattices, it can be shown that these states are stable if the following condition is satisfied [18, 29],

$$\left| \left(1 - \varepsilon + \frac{\varepsilon}{N} m_k \right) e^\lambda \right| < 1, \quad (4)$$

where $\{m_k : k = 1, 2, \dots, N\}$ is the set of eigenvalues of the coupling matrix \mathbf{M} and λ is the Lyapunov exponent of the local map, Ec. (2). In the globally coupled case, the eigenvalues are $m_k = 0$, $k = 1, \dots, (N - 1)$, which has $(N - 1)$ -fold degeneracy, and $m_N = N$. Because of these eigenvalues, the synchronization condition, Ec. (4), is independent of the size of the system N .

The set of eigenvectors of the matrix \mathbf{M} constitute a complete orthogonal basis in terms of which any state \mathbf{x}_t of the system Ec. (3) can be represented as a linear combination. The eigenvector corresponding to $m_N = N$ is homogeneous and it expresses the coherent or synchronized state at any time. Thus, perturbations of the state \mathbf{x}_t along this eigenvector do not destroy the coherence, and the stability condition associated with $m_N = N$ is irrelevant for the synchronized state. The other $(N - 1)$ eigenvectors associated with $m_k = 0$ are not homogeneous, and perturbations along their directions affect the synchronized state. Thus, the stability condition Ec. (4) with $m_k = 0$ defines a region on the space of parameters (μ, ε) where all the stable synchronized states can be found.

Two types of synchronized states fulfilling condition Ec. (4) can be observed in the system:

1. Synchronized stationary states, for which $x_t^i = x^*$, $\forall i$. This corresponds to the range of parameter $\mu \in [-1, 1]$, where the local map possesses the stable fixed point $f(x^*) = x^* = 0$. The boundaries of the region of parameters where this state is stable are given by Ec. (4) with $m_k = 0$ and $e^\lambda = f'(x^*)$,

$$(1 - \varepsilon) |f'(x^*)| = \pm 1. \quad (5)$$

2. Synchronized chaotic states, for which $x_t^i = f(x_t)$, $\forall i$. This occurs in the regions $\mu \in [-3, -1] \cup [1, 3]$, where the local map is chaotic. The region of stability of these states is bounded by the curves

$$(1 - \varepsilon) e^\lambda = \pm 1, \quad (6)$$

Since $f'(x^*) = \mu$ and $\lambda = \ln |\mu|$ for the map Ec. (2), both boundaries (5) and (6) can be expressed on the space of parameters (μ, ε) by the curves

$$(1 - \varepsilon) |\mu| = \pm 1, \quad (7)$$

with μ in the appropriate range for each state. The straight lines $\mu = -1$ and $\mu = 1$ separate the synchronized stationary states from the synchronized chaotic states on the plane (μ, ε) .

The occurrence of synchronization can also be numerically characterized by the asymptotic time-average $\langle \sigma \rangle$ (after discarding a number of transients) of the instantaneous standard deviations σ_t of the distribution of state variables x_t^i , defined as

$$\sigma_t = \left[\frac{1}{N} \sum_{i=1}^N (x_t^i - \bar{x}_t)^2 \right]^{1/2}, \quad (8)$$

where

$$\bar{x}_t = \frac{1}{N} \sum_{i=1}^N x_t^i. \quad (9)$$

Then, a synchronization state corresponds to a value $\langle \sigma \rangle = 0$. In practice, we use the numerical criterion $\langle \sigma \rangle < 10^{-7}$ as a synchronization condition.

For some values of parameters, the iterates of the state variables x_t^i in the system Ec. (1) leave the interval $[-1, 1]$ and, eventually, escape to infinity. The iterates of x_t^i stay in the interval $[-1, 1]$ if the product $(1 - \varepsilon)\mu$ lies in the range $[-3, 3]$; that is if $|(1 - \varepsilon)\mu| < 3$. Thus, the boundaries for escape from the interval $[-1, 1]$ are described by the curves

$$(1 - \varepsilon) \mu = \pm 3. \quad (10)$$

Figure (1) shows the stability boundaries of the synchronized states and the escape boundaries for the globally coupled system Ec. (1) on the space of parameters (μ, ε) .

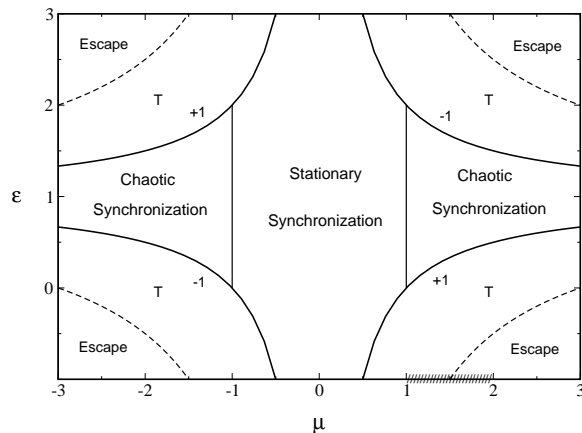


FIG. 1: Regions of stable synchronized states for the system Ec. (1) on the space of parameters (μ, ε) . The labels indicate where the synchronized stationary states and the synchronized chaotic states occur. The synchronization boundaries correspond to continuous lines. The labels ± 1 on each curve identify the corresponding sign in Ec. (7). The dashed lines indicate the escape boundaries Ec. (10) beyond which the iterates of the state variables of the system Ec. (1) leave the interval $[-1, 1]$. The interval $\mu \in [1, 2]$ for bistability is marked on the μ axis. The label T identifies the regions where collective turbulent states exist.

IV. COLLECTIVE PHASES.

For $\mu \in (1, 2)$, the local map displays bistability in the form of two chaotic band attractors: corresponding to the interval I^+ for the positive values of the iterates, and the interval I^- for the negatives values. Then the states of the elements in the system Ec. (1) can be associated to two well defined symmetric phases that can be characterized by spin variables associated to the sign of the state at time t , defined as $s_t^i = +1$ if $x_t^i > 0$, and $s_t^i = -1$ if $x_t^i < 0$.

To study the collective behavior of the globally coupled map system Ec. (1) in the bistable chaotic range, we fix the value of the local parameter $\mu = 1.9$ and choose an even number N as system size. Then we set the initial conditions symmetrically as follows: one half of the maps are randomly chosen and assigned random values uniformly distributed on the positive attractor while the other half are similarly assigned values on the negative attractor.

The dynamical properties of the phase-ordering process can be described by using the persistence probability p_t , defined as the fraction of maps that have not changed spin variable (sign) up to time t [30]. Figure (2) shows p_t as a function of time for the globally coupled map system Ec. (1), for several values of the coupling parameter ε . The persistence probability saturates in a few iterations for all positive values of the coupling ε . This means that the phases associated to the spin variables freeze in the globally coupled system. In contrast, in regular lattices the persistence saturates for small couplings, while it decays algebraically in time for coupling strengths greater than some critical value, corresponding to the growth of one phase at the expense of the other [21].

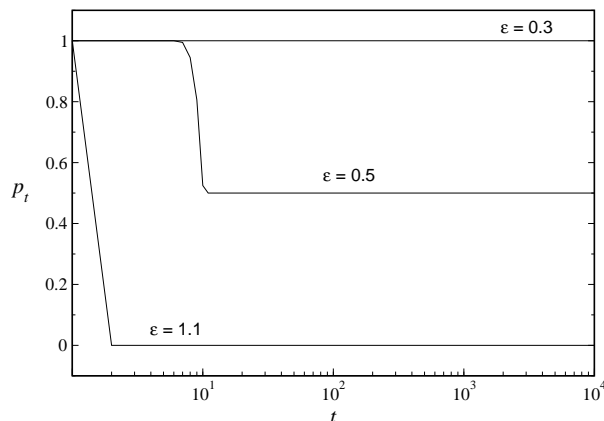


FIG. 2: Persistence probability as a function of time for the system Ec. (1) with fixed $\mu = 1.9$ and size $N = 10^5$, for different values of the coupling parameter ε , as indicated on each curve.

Figure (2) reveals that the saturation value of the persistence probability, denoted by p_∞ , depends on the value of the coupling parameter. Figure (3a) shows the quantity p_∞ as a function of ε . We find that p_∞ displays different constant values in different intervals of the coupling parameter and exhibits discontinuous transitions at critical values $\varepsilon_1 = 0.43$ and $\varepsilon_2 = 1$. For $\varepsilon < \varepsilon_1$, we have $p_\infty = 1$, indicating that for small enough coupling, every map remains in its initial chaotic attractor, I^- or I^+ . In the intermediate range of coupling parameters $\varepsilon_1 < \varepsilon < 1$, the saturation value of the persistence changes to $p_\infty = 0.5$, indicating that one-half of the total number of maps have switched attractor. Finally, for $\varepsilon > 1$, we obtain $p_\infty = 0$; this means that all the maps have changed their initial attractors at some time during the evolution of the system. The value of ε_1 depends on the value of the local map parameter μ , but $\varepsilon_2 = 1$, independently of μ .

Figure (3b) shows the synchronization measure $\langle \sigma \rangle$, given by Eq. (8), as a function of ε . For the value $\mu = 1.9$, the chaotic synchronization range of the coupling, obtained from Eq. (7), is $\varepsilon \in [0.473, 1.526]$. For this interval of the coupling, we get $\langle \sigma \rangle = 0$ as expected.

To characterize the statistical properties of the phase-ordering process in the globally coupled map system Ec. (1), we define the instantaneous “magnetization” of the system M_t , as

$$M_t = \frac{1}{N} \sum_{i=1}^N s_t^i. \quad (11)$$

Then, we employ, as an order parameter, the absolute value of the asymptotic time-average (after discarding a number of transients) of the values M_t , denoted by $\langle M \rangle$.

Figure (3c) shows the order parameter $\langle M \rangle$ as a function of the coupling ε . The critical value of the coupling ε_1 marks a discontinuous transition from a collective state characterized by $\langle M \rangle = 0$, where the maps remain symmetrically

distributed about the two attracting intervals I^+ and I^- , to an ordered state characterized by $\langle M \rangle = 1$, where all the maps settle on one of the attractors, either I^+ or I^- . Note that the critical value ε_1 is smaller than the lower synchronization boundary at $\varepsilon = 0.473$. This means that the phase-ordering transition occurs before full synchronization is achieved. When the value of the coupling strength reaches the upper synchronization boundary, there is another discontinuous transition to the turbulent, disordered state, for which $\langle M \rangle = 0$.

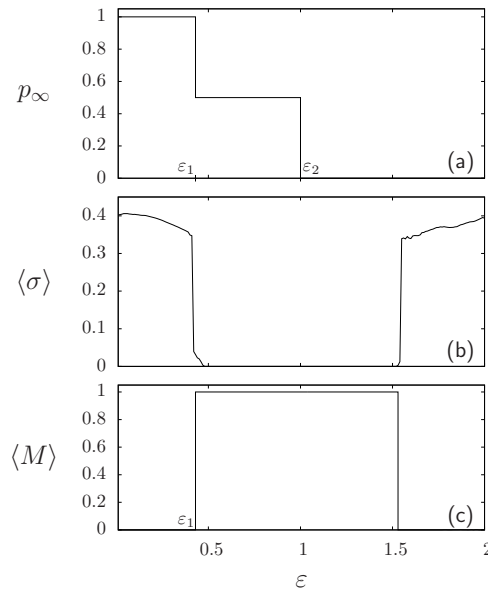


FIG. 3: Statistical quantities as functions of the coupling parameter ε for system Ec. (1) with fixed $\mu = 1.9$ and size $N = 10^5$. (a) p_∞ ; (b) $\langle \sigma \rangle$; (c) $\langle M \rangle$. The critical values ε_1 and ε_2 are marked on the ε axis.

The quantities p_∞ and $\langle \sigma \rangle$ in Fig. (3) allow to distinguish three different situations in the range of the parameter ε where the collective phase-ordered state with $\langle M \rangle = 1$ occurs: (i) a desynchronized ordered state, where $\langle M \rangle = 1$, $\langle \sigma \rangle > 0$, and $p_\infty = 0.5$; (ii) a synchronized ordered state, where $\langle M \rangle = 1$, $\langle \sigma \rangle = 0$, and $p_\infty = 0.5$; and (iii) a synchronized ordered state, characterized by $\langle M \rangle = 1$, $\langle \sigma \rangle = 0$, and $p_\infty = 0$.

In order to elucidate the nature of these three realizations of the phase-ordered state, as well as the transitions exhibited by the statistical quantities p_∞ and $\langle M \rangle$, we plot in Fig. (4) the instantaneous probability distributions of the states x_t^i of the system Eq. (1) with fixed $\mu = 1.9$, denoted by $\rho(x)$, for different values of the coupling parameter ε .

Figure (4a) corresponds to $\varepsilon = 0.2 < \varepsilon_1$. The probability distribution $\rho(x)$ at $t = 2000$ shows two separated peaks that maintain the initial symmetrical distribution of the maps on the two chaotic band attractors. The mean field coupling term is negligible in this situation Figure (5a) shows the time evolution of the state variables x_t^i of two maps in the system Ec. (1) for $\varepsilon = 0.2$: one having positive initial spin variable and another with negative initial spin variable. Each trajectory remains in its attractor. Since no map has left its initial attractor, no spin variable has changed sign, and thus $p_\infty = 1$. Then, two symmetric subsets associated to the spin variables coexist in the globally coupled system for these parameters values, yielding $\langle M \rangle = 0$ as a result.

For couplings $\varepsilon_1 < \varepsilon < 0.473$ in Fig. (4b), the probability distribution $\rho(x)$ at time $t = 2000$ displays one single peak. This indicates that the $N/2$ maps that initially belonged to one attractor have switched to the other attractor; the direction of the change depends on the initial conditions, in this case from I^- to I^+ . All the maps form a cluster that moves chaotically and stays in the interval I^+ . Then, the saturation value of the persistence probability is $p_\infty = 0.5$ in this range of the coupling strength. Figure (5b) illustrates this process through the time evolution of the orbits of two maps that have been initially assigned opposite spin variables. Note that the two chaotic orbits do not synchronize on the interval I^+ . This situation corresponds to the presence of a single ordered phase of spin variables in the system, and therefore the magnetization becomes $\langle M \rangle = 1$. The discontinuous change in the statistical quantities occurring at the critical value ε_1 in Fig. (3) describes a first order phase transition in the collective behavior of the system, from a non-ordered state, characterized by the values $\langle \sigma \rangle > 0$, $p_\infty = 1$, $\langle M \rangle = 0$, to a desynchronized phase-ordered state, characterized by $\langle \sigma \rangle > 0$, $p_\infty = 0.5$, $\langle M \rangle = 1$, and denoted as situation (i) above.

For coupling values $0.473 < \varepsilon < 1$, the probability $\rho(x)$ at $t = 2000$ displays a single vertical line on one of the attracting intervals, as shown in Fig. (4c). This indicates that the $N/2$ maps initially assigned to one of the attractors have switched to the other attractor, resulting in the synchronization of the N maps on a single chaotic orbit that

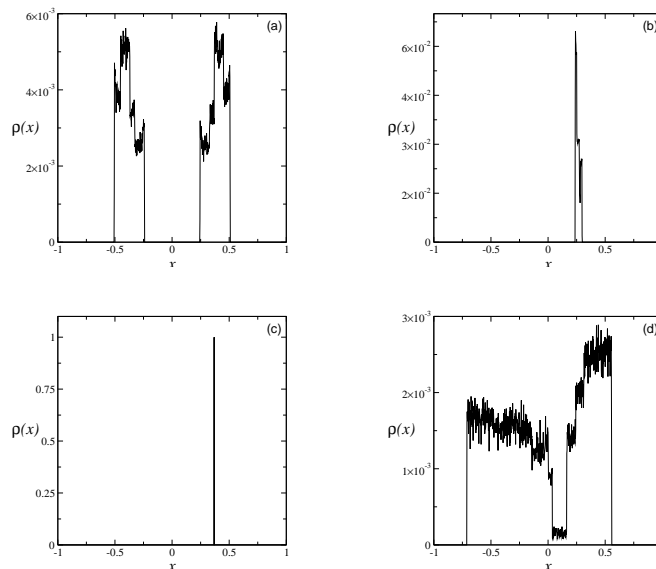


FIG. 4: Instantaneous probability distributions $\rho(x)$ of states at time $t = 2000$ for the system Ec. (1) with $N = 10^5$ and fixed $\mu = 1.9$, for different values of the coupling ε . (a) $\varepsilon = 0.2$ (non-ordered phase, $p_\infty = 1$, $\langle M \rangle = 0$), (b) $\varepsilon = 0.45$ (desynchronized ordered phase, $\langle \sigma \rangle > 0$, $p_\infty = 0.5$, $\langle M \rangle = 1$), (c) $\varepsilon = 0.55$ (synchronized ordered phase, $\langle \sigma \rangle = 0$, $p_\infty = 0.5$, $\langle M \rangle = 1$). (d) $\varepsilon = 2.4$ (turbulent).

stays on that attractor. The corresponding time evolution of two maps with initial opposite spin variables is shown in Fig. (5c). Thus, the system displays a synchronized, phase-ordered state characterized by $\langle \sigma \rangle = 0$, $p_\infty = 0.5$, and $\langle M \rangle = 1$ in this parameter range. This constitutes realization (ii) of the phase-ordered state.

If the coupling is increased to values $1 < \varepsilon < 1.526$, we observe realization (iii) of the ordered state. In this case, the factor $(1 - \varepsilon)$ in Ec. (1) becomes negative allowing the maps to reverse the signs of their initial spin variables at early times during the evolution of the system. This transient behavior of the spin variables is reflected in the quantity $p_\infty = 0$; the parameter $\varepsilon_2 = 1$ marks the discontinuity in the value of the saturation value of the persistence. Since the synchronized state is stable for this range of coupling parameters, the maps eventually become synchronized on one of the attracting intervals, yielding $\langle \sigma \rangle = 0$. In addition, we obtain $\langle M \rangle = 1$. Figure (5d) portrays the time evolution of the orbits of two maps with different initial spin variables in this situation. Then, we have again a synchronized, phase-ordered state, distinguished by the value $p_\infty = 0$, in contrast to realization (ii) where $p_\infty = 0.5$. Thus, the saturation value of the persistence probability can provide information about the transient processes that lead to frozen configurations and to phase-ordered states in the system.

In Fig. (4d) for $\varepsilon > 1.526$, the maps become desynchronized and the corresponding probability distribution $\rho(x)$ is spread over a subset of the interval $x \in [1, 1]$; its bimodal form reflects the underlying presence of the two attractors in the local chaotic dynamics. We refer to this collective state as turbulent. This corresponds to a desynchronized, disordered state for which $\langle \sigma \rangle > 0$, $p_\infty = 0$, and $\langle M \rangle = 0$.

If the initial conditions are modified in such a way that a fraction $N_1/N > 1/2$ of values of the maps is uniformly distributed on one attractor interval, either I^+ or I^- , while the remaining fraction $(1 - N_1/N)$ is similarly assigned to the other attractor, then the symmetry of the globally coupled system Ec. (1) is lost. We have found that the main features of the collective behavior of the system are maintained under such partition: the persistence probability p_t saturates after a few iterations for all values of the coupling parameter; there is a disordered state for low coupling values; and a synchronized phase-ordered state emerges for an intermediate range of the coupling strength.

In this situation, the mean field of the system initially acquires the sign of the attractor where the largest fraction N_1/N of maps lies. This attractor dominates the dynamics of the globally coupled bistable system. However, for low enough intensity of the coupling, the maps tend to stay in their initial intervals and therefore they do not change the sign of their spin variable. Correspondingly, the asymptotic persistence probability has the value $p_\infty = 1$ and the average magnetization is $\langle M \rangle = 0$. As the coupling strength is increased, the maps in the smallest subset switch to the dominating attractor, eventually giving rise to a phase-ordered state. The initial fraction of maps N_1/N remain on that attractor and therefore do not change sign in their spin variables. Then, the saturation value of the persistence probability for ordered state in this case should be $p_\infty = N_1/N$. We have numerically verified these values for different partitions $(N_1, N - N_1)$ of initial conditions over the attracting intervals.

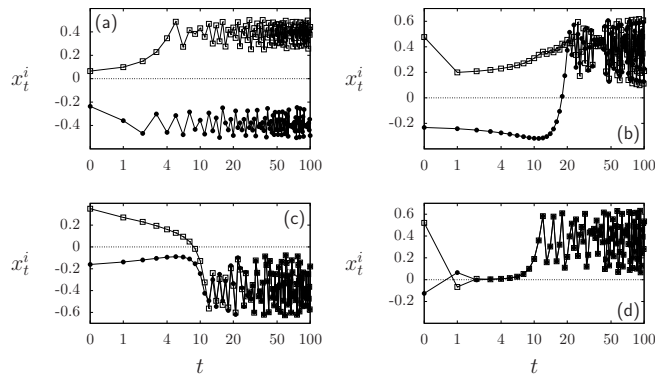


FIG. 5: Temporal evolution of the state variables x_t^i of a map with positive initial spin variable (empty squares) and a map with negative initial spin variable (black circles) in the globally coupled system Ec. (1) with $N = 10^5$ and fixed $\mu = 1.9$, for different values of the coupling ε . For $t > 0$, time is displayed in a logarithmic scale. (a) $\varepsilon = 0.2$; non-ordered state, with $\langle \sigma \rangle > 0$, $p_\infty = 1$, $\langle M \rangle = 0$. (b) $\varepsilon = 0.45$; desynchronized, ordered state, with $\langle \sigma \rangle > 0$, $p_\infty = 0.5$, $\langle M \rangle = 1$. (c) $\varepsilon = 0.55$; synchronized, ordered state, with $\langle \sigma \rangle = 0$, $p_\infty = 0.5$, $\langle M \rangle = 1$. (d) $\varepsilon = 1.1$; synchronized, ordered state, with $\langle \sigma \rangle = 0$, $p_\infty = 0$, $\langle M \rangle = 1$.

V. CONCLUSIONS.

We have investigated the collective behavior of a system of globally coupled maps having bistable, chaotic local dynamics. The system possesses two types of synchronized dynamics: synchronized stationary states and synchronized chaotic states. We have analytically determined the stability boundaries of these states on the space of parameters (ε, μ) of the system. In addition, we have numerically measured the occurrence of synchronization by means of the statistical quantity $\langle \sigma \rangle$.

The presence of two symmetric attracting intervals in the local chaotic dynamics permits to assign a spin-like variable to each map and to define associated phases. The persistence probability p_t describes the evolution and competition of the phases. The absence of spatial relations in the system of globally coupled maps rules out the possibility of supporting spatial domains in either phase and a defined interface which would be necessary for a continuous phase growth. As a consequence, the phases always freeze in globally coupled maps, causing the saturation of the persistence probability in time for all values of the coupling parameter, in contrast to the transition observed in the temporal behavior of the persistence in coupled maps on regular lattices. We have found that the saturation value of the persistence probability p_∞ reaches different constant values in different intervals of the coupling parameter and shows discontinuous transitions at critical values $\varepsilon_1 = 0.43$ and $\varepsilon_2 = 1$.

We have introduced the magnetization-like order parameter $\langle M \rangle$ to characterize the phase-ordering behavior of the system. The phase-ordered state, corresponding to $\langle M \rangle = 1$, exhibits three distinct realizations as the coupling ε is varied and which can be discerned by employing the quantities $\langle \sigma \rangle$ and p_∞ : (i) a desynchronized ordered state, with $\langle M \rangle = 1$, $\langle \sigma \rangle > 0$, and $p_\infty = 0.5$; (ii) a synchronized ordered state, characterized by $\langle M \rangle = 1$, $\langle \sigma \rangle = 0$, and $p_\infty = 0.5$; and (iii) a synchronized ordered state, distinguished by $\langle M \rangle = 1$, $\langle \sigma \rangle = 0$, and $p_\infty = 0$. Thus, the value of $\langle \sigma \rangle$ distinguishes between realizations (i) and (ii); while p_∞ differentiates realization (ii) from realization (iii).

There also exist two desynchronized, non-ordered collective states, both described by the values $\langle \sigma \rangle > 0$ and $\langle M \rangle = 0$. One of these states corresponds to the persistence of the initial symmetric distribution of spin variables, characterized by $p_\infty = 1$; and the other is a turbulent state, where $p_\infty = 0$. Our results reveal that the saturation value of the persistence probability can provide information about the transient behaviors that lead to the different phase configurations in the system.

In addition, we have studied the histograms and the time evolution of local map variables associated to the disordered and to the phase-ordered states in order to understand the appearance of these collective states in the globally coupled system. The transitions between the disordered states and the phase-order state occur discontinuously, as in a first-order phase transition, reflecting the global nature of the interaction in the system. In contrast, continuous transitions are typical in regular lattices.

In general, the investigation of dynamical processes in networks and the role of the topology in determining emerging collective behaviors is a topic of much interest in the current research on complex systems [8, 31].

Acknowledgements

This work is supported by project No. C-1827-13-05-B from CDCHTA, Universidad de Los Andes, Venezuela. M. G. C. is grateful to the Senior Associates Program of the Abdus Salam International Centre for Theoretical Physics, Trieste, Italy.

-
- [1] Wiesenfeld, K., Hadley, P.: Attractor crowding in oscillator arrays. *Phys. Rev. Lett.* **62**, 1335–1338 (1989).
 - [2] Wiesenfeld, K., Bracikowski, C., James, G., Roy, R.: Observation of antiphase states in a multimode laser. *Phys. Rev. Lett.* **65**, 1749–1752 (1990).
 - [3] Kuramoto, Y.: *Chemical Oscillations, Waves and Turbulence*. Springer, Berlin (1984).
 - [4] Nakagawa N., Kuramoto, Y.: From collective oscillations to collective chaos in a globally coupled oscillator system. *Physica D* **75**, 74–80 (1994).
 - [5] G. Grüner: The dynamics of charge-density waves. *Rev. Mod. Phys.* **60**, 1129–1181 (1988).
 - [6] Kaneko K., Tsuda, I.: *Complex Systems: Chaos and Beyond*. Springer, Berlin (2001).
 - [7] Yakovenko, V.M. In: *Encyclopedia of Complexity and System Science*, edited by Meyers, R.A. Springer, New York (2009).
 - [8] Newman, M., Barabási, A.L., Watts, D.J.: *The Structure and Dynamics of Networks*. Princeton University Press, Princeton (2006).
 - [9] González-Avella, J.C., Eguiluz, V.M., Cosenza, M.G., Klemm, K., Herrera, J.L., San Miguel, M.: Local versus global interactions in nonequilibrium transitions: A model of social dynamics. *Phys. Rev. E* **73**, 046119 (2006).
 - [10] González-Avella, J.C., Cosenza, M.G., San Miguel, M.: A model for cross-cultural reciprocal interactions through mass media. *PLoS One* **7**(12), e51035 (2012).
 - [11] Manrubia, S.C. Mikhailov, A.S., Zanette, D.H.: *Emergence of Dynamical Order: Synchronization Phenomena in Complex Systems*. World Scientific, Singapore (2004).
 - [12] Garcia-Ojalvo, J., Elowitz, M.B., Strogatz, S.H.: Modeling a synthetic multicellular clock: Repressilators coupled by quorum sensing. *Proc. Natl. Acad. Sci. U.S.A.* **101**, 10955–10960 (2004).
 - [13] Wang, W., Kiss, I.Z., Hudson, J.L.: Experiments on arrays of globally coupled chaotic electrochemical oscillators: Synchronization and clustering. *Chaos* **10**, 248–256 (2000).
 - [14] Miyakawa, K., Yamada, K.: Synchronization and clustering in globally coupled salt-water oscillators. *Physica D* **151**, 217–227 (2001).
 - [15] De Monte, S., dOvidio, F., Danø, S., Sørensen, P.G.: Dynamical quorum sensing. *Proc. Natl. Acad. Sci. U.S.A.* **104**, 18377–18381 (2007).
 - [16] Taylor, A.F., Tinsley, M.R., Wang, F., Huang, Z., Showalter, K.: Dynamical quorum sensing and synchronization in large populations of chemical oscillators. *Science* **323**, 614–617 (2009).
 - [17] Hagerstrom, A.M., Murphy, T.E., Roy, R., Hövel, P., Omelchenko, I., Schöll, E.: Experimental observation of chimeras in coupled-map lattices. *Nature Phys.* **8**, 658–661 (2012).
 - [18] Kaneko, K.: Clustering, coding, switching, hierarchical ordering, and control in networks of chaotic elements. *Physica D* **41**, 137–172 (1990).
 - [19] Miller, J., Huse, D.A.: Macroscopic equilibrium from microscopic irreversibility in a chaotic coupled map lattice. *Phys. Rev. E*, **48**, 2528–2535 (1993).
 - [20] O’Hern, C., Egolf, D., Greenside, H.S.: Lyapunov spectral analysis of a nonequilibrium Ising-like transition. *Phys. Rev. E* **53**, 3374–3386 (1996).
 - [21] Lemaître, A., Chaté, H.: Phase ordering and onset of collective behavior in chaotic coupled map lattices. *Phys. Rev. Lett.*, **82**, 1140–1143 (1999).
 - [22] Kockelkoren, J., Lemaître, J., Chaté, H.: Phase-ordering and persistence: relative effects of space-discretization, chaos, and anisotropy. *Physica A* **288**, 326–337 (2000).
 - [23] Wang, W., Liu, Z., Hu, B.: Phase order in chaotic maps and coupled map lattices. *Phys. Rev. Lett.* **84**, 2610–2613 (2000).
 - [24] Schmüser, F., Just, M., Kantz, H.: On the relation between coupled map lattices and kinetic Ising models. *Phys. Rev. E* **61**, 675–3684 (2000).
 - [25] Angelini, L., Pellicoro, M., Stramaglia, S.: Phase ordering in chaotic map lattices with additive noise. *Phys. Lett. A* **285**, 293–300 (2001).
 - [26] Angelini, L.: Antiferromagnetic effects in chaotic map lattices with a conservation law. *Phys. Lett. A* **307**, 41–49 (2003).
 - [27] Tucci, K., Cosenza, M.G., Alvarez-Llamoza, O.: Phase separation in coupled chaotic maps on fractal networks. *Phys. Rev. E* **68**, 027202 (2003).
 - [28] Echeverria, C., Tucci, K., Cosenza, M.G.: Phase growth in bistable systems with impurities. *Phys. Rev. E* **77**, 016204 (2008).
 - [29] Waller, I. Kapral, R.: Spatial and temporal structure in systems of coupled nonlinear oscillators. *Phys. Rev. A*, **30**, 2047–2055 (1984).
 - [30] Derrida, B., Bray, A.J., Godrèche, C.: Non-trivial exponents in the zero temperature dynamics of the 1d Ising and Potts model. *J. Phys. A* **27**, L357–L361 (1994).
 - [31] Herrera, J.L., Cosenza, M.G., Tucci, K., González-Avella, J.C.: General coevolution of topology and dynamics in networks.

Europhys. Lett. **95**, 58006 (2011).